Acta Geodyn. Geomater., Vol. 8, No. 4 (164), 425–441, 2011

# THE IDENTIFICATION OF FAULTS USING MORPHOSTRUCTURAL AND GEOPHYSICAL METHODS: A CASE STUDY FROM STRAŠÍN CAVE SITE

**Filip HARTVICH * and Jan VALENTA**

*Institute of Rock Structure and Mechanics, Academy of Sciences of the Czech Republic, v.v.i.,*
*V Holešovičkách 41, 182 09 Prague, Czech Republic*
**Corresponding author's e-mail:* hartvich@irsm.cas.cz

(*Received* March 2011, *accepted* July 2011)

**ABSTRACT**
This paper combines morphostructural analysis and geophysical methods in order to link the faults monitored inside Strašín Cave with faults and lineaments in the vicinity of the cave. The studied site is situated in SW Bohemia, at the foothills of the Bohemian Forest Mts. Main goal is to combine the morphostructural, morphometrical and geophysical methods in order to identify the fault system, monitored inside the cave. This will allow relevant interpretation of the observed movements in the frame of the local tectonic environment. The results show that the monitored faults are observable in the geophysical profiles and, using our knowledge of the structural setting, we have been able to link them with mapped tectonic structures in the vicinity of the cave. Thus, it has been demonstrated that even where outcrops are absent, the faults can be traced and that the monitored faults are significant enough to yield relevant data on tectonic movements. In addition, the combined resistivity and gravimetry profiles reveal a possible new, presently unknown, cave located 20 m below the surface about 200 m north-northeast of Strašín Cave.

**KEYWORDS:** geophysical profiling, morphostructural analysis, cave, faults, Bohemian Forest Mts.

## 1. INTRODUCTION

The monitoring of faults in caves has become widely used in studies of active tectonic movements (Stemberk et al., 2003; Briestenský et al., 2010; Stemberk and Hartvich, 2011). The use of caves has numerous advantages: relative protection (particularly in locked caves), stable temperatures, and the simple identification of active faults as indicated by ruptures in flowstone. However, caves with (observed) faults represent only rare and often unique points in the geological environment. Therefore, to be able to interpret the observed movements within the context of the morphostructural "neighbourhood", it is necessary to link the faults in the caves to those identified by morphostructural or geological mapping in the surrounding area.

This is not as straightforward as it may seem. First, not all the existing faults (and, in fact, very few) have clear traces on the surface as indicated by striated outcrops, dyke fillings, or manifestations in the relief; thus, not all existing faults are recorded in maps. Second, even if they can be revealed by a detailed study, not all have been recorded in common general mapping. In the case of the Czech Republic, this is undertaken at the rather rough scale of 1:50 000. Third, even if the faults are recorded in the general geological maps, their exact course is rarely confirmed by excavation, drilling, or geophysical research. This is usually due to the significant cost of undertaking these methods.

Geophysical methods are commonly used for geological mapping, primarily in areas covered by vegetation and Quaternary sediments. In such areas, geological mapping is a very demanding task and results are often disputable (Abu Shariah, 2009). The geophysical measurements can, in many cases, give additional information able to prove or reject questionable theories (Schrott and Sass, 2008).

For many years, geoelectric resistivity methods have been commonly used in the search for discontinuities. With advances in electronics, devices have become more accurate and capable of delivering much finer information on sub-surface composition. This is frequently exploited in archaeological (Burger, 1992; Abu Shariah, 2009), geological, and geomorphological research (Schrott and Sass, 2008; Skácelová et al., 2010). Recently, it has begun to be used to document known, and search for undiscovered, underground spaces (Guerin et al., 2009; Pánek et al., 2010). Sometimes this is done in combination with other geophysical methods (Abu Shariah 2009).

### *1.1. GEOLOGICAL AND MORPHOSTRUCTURAL SETTINGS*

Strašín Cave is situated in the Pošumavský Karst (a part of the Varied series in Fig. 1), which comprises a belt of fragmented blocks of metamorphic crystalline limestones and dolomites set inside predominating biotitic paragneisses (Kukla and

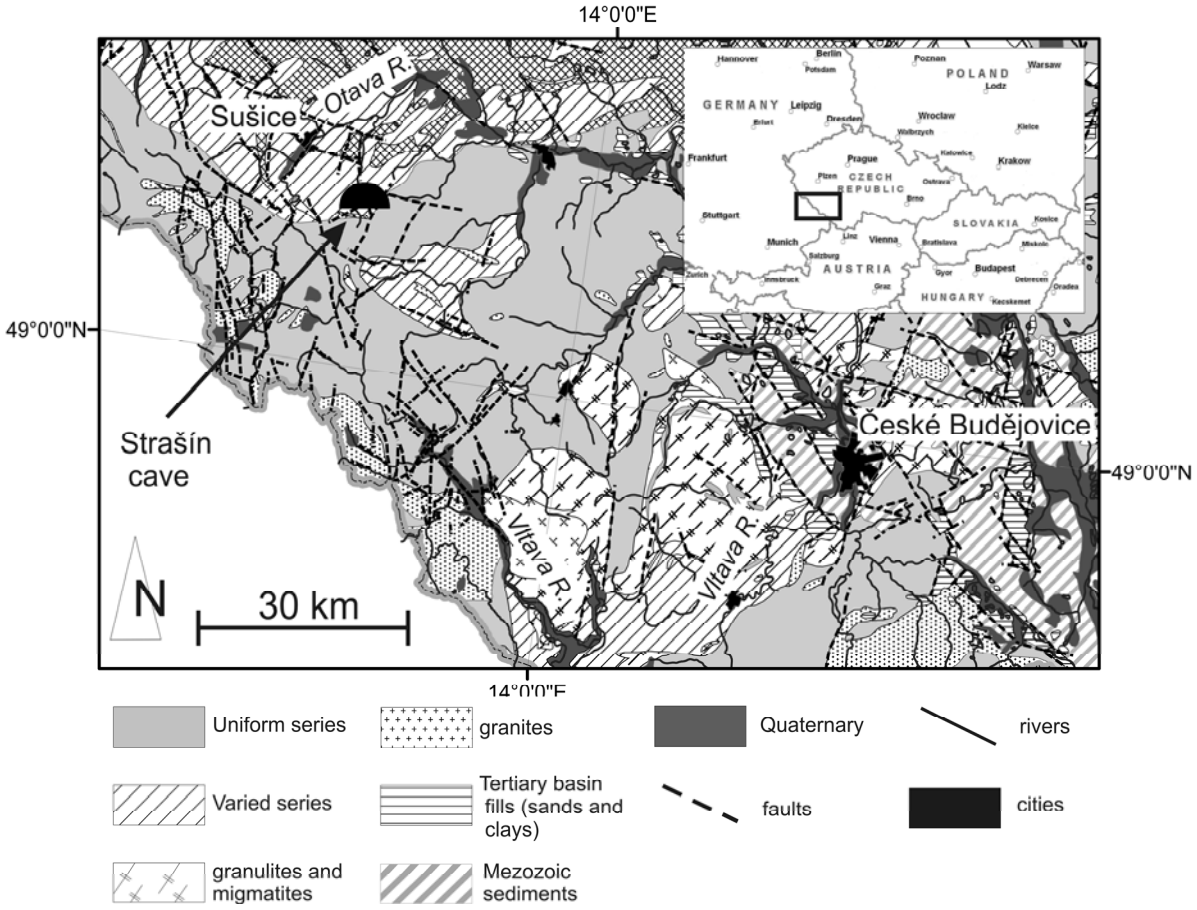


**Fig. 1** Position of the studied region around the Strašín cave site (indicated by black arrow) in central Europe and in the Czech Republic with a simplified geological map (after Čech et al., 1962 and Kodym et al., 1961).

Skřivánek, 1954). These often elongated lenses of limestones are part of the Varied Series of the Moldanubicum Unit, a consolidated crystalline unit consisting mostly of gneisses with various insets and a few granitic plutons. This unit forms the bedrock of southern and southwestern Bohemia (Čech et al., 1962; Babůrek et al., 2006). The other is called the Uniform Series, which contains a smaller amount of intrusions and sedimentary insets.

Strašín Cave has developed in a limestone of medium coarseness with grains typically 1-1.5 mm. The limestone body has a crescent-like shape, elongated NW-SE, with a length of approximately 300 m. The limestones of the Varied Series are typically strongly tectonically fractured as a result of a long deformation history (Babůrek et al., 2001).

## 2. METHODS

### *2.1. STRUCTURAL AND MORPHOLOGICAL RESEARCH*

To be able to fit the observed faults into the structural setting of the surrounding region of Pošumaví, it was necessary to analyse tectonic features based on both the known faults derived from geological maps and the properties of the relief which can often reveal hidden structures. The faults are often associated with typical morphological features such as valleys, ridges, and linear slopes. These can be observed using various analyses of a DEM (Jordan and Schott, 2005).

The surrounding area was delimited into five catchments along the slopes of the Bohemian Forest Mts. (Fig. 2) including the Nezdický and Podmokelský streams, with a neighbouring segment of the Otava River, Mačický, Novosedelský, and Peklov streams. The total area under consideration is 292 sq. km. The catchments were chosen as well-defined functional units of the relief (Křížek et al., 2006) and delimited in accordance with the regional geomorphological units (Balatka and Kalvoda, 2005). All the morphological and morphostructural analyses were undertaken in this area of interest. The directions of the datasets were analysed both visually and statistically, using Spearman's rank correlation coefficient (c.f. Štěpančíková, 2007).

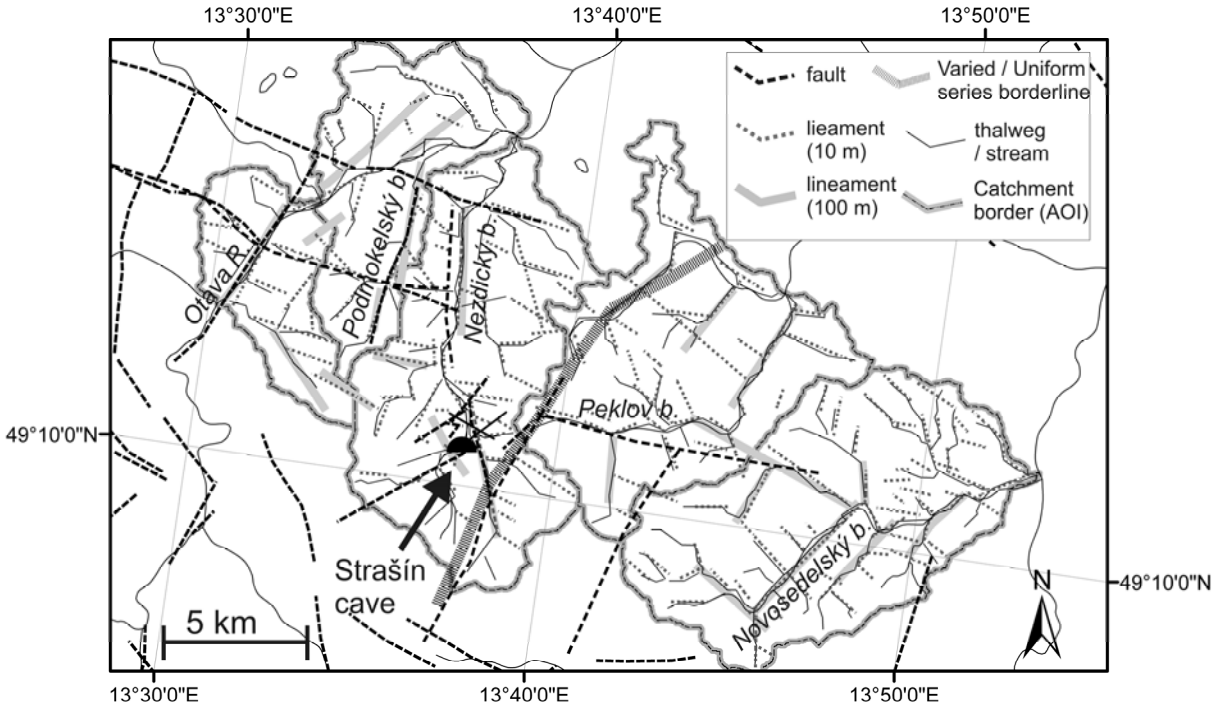


**Fig. 2** Map of the Area of Interest (AOI) used for morphostructural analysis showing the morpholineaments, main faults and analysed thalwegs.

The first analysis examined morpholineaments (or sometimes called also topographic lineaments). These are linear elements of the relief as described by, for example, Koike et al. (1998), Casas et al. (2000), Štěpančíková (2007), Ekneligoda and Henkel (2010), and Minár et al. (2010). Two sets of lineaments were used: the first was drawn from the visual analysis of shaded 10 m DEM (Casas et al., 2000; Jordan et al., 2005); the second was created from a coarser 100 m DEM.

Since the advent of GIS, many methods for the analysis of lineaments have been developed (Clark and Wilson, 1994; Raghavan et al., 1995; Casas et al., 2000; Ekneligoda and Henkel, 2010). However, no reliable technique has fully managed the automatic drawing of such lineaments. There are, however, methods that can aid the investigator, such as construction of a raster of linear forms, used in this study. It is calculated as a neighbourhood analysis (majority) of Thiessen polygons based on the centrepoints of 100 m segments of contour lines where the value was represented by the azimuth of each contour line segment. This raster highlights the linear elements of the relief and thus helps to define the lineaments.

The analysis of valley segments within the area of interest used the stream layer from the 1:10 000 digital vector map ZABAGED. In the study area, this layer comprises 365 km of rivers and streams. The layer was split into 1 km segments to avoid the blurring of the results by non-structural influences such as natural river meandering or artificial channel changes.

A set of known faults was extracted from the geological map at the scale of 1:50 000 (Pelc and Šebesta, 1994; Müller et al., 1999) and at the scale 1:25 000 (Babůrek et al., 2001). Altogether, only 11 fault structures have been recorded in the study area with a total length of 38 km. The tectonic fracturing was measured inside the cave as well as on the limestone outcropping on the surface. Some data on the joint system were also taken from Kukla and Skřivánek (1954), who measured several structures in the cave.

Finally, the analysis of the large, elongated, slopes (or large linear slopes, LLS) was undertaken. Again, this was based on the 10 m DEM. A map of slope aspect was reclassified into 8 categories, each representing a generalised direction (N, NE, E, SE, S, SW, W, NW). The reclassified raster was converted into a polygon layer and geometrical parameters were calculated for each object using ET Geowizards: length, width, thickness, circularity, perimeter, and area. Then the selection was refined so that polygons that were too small (less than 0.25 sq. km) and too wide (length/width ratio less than 4) were removed as well as those with the highest perimeter/area ratio. The limit values for the geometrical properties were set to 3rd percentile (75 %) of each set. Thereafter, only the 140 largest, simplest, and most elongated polygons remained. For these, the longest axis was drawn and its azimuth and length calculated (Fig. 3).

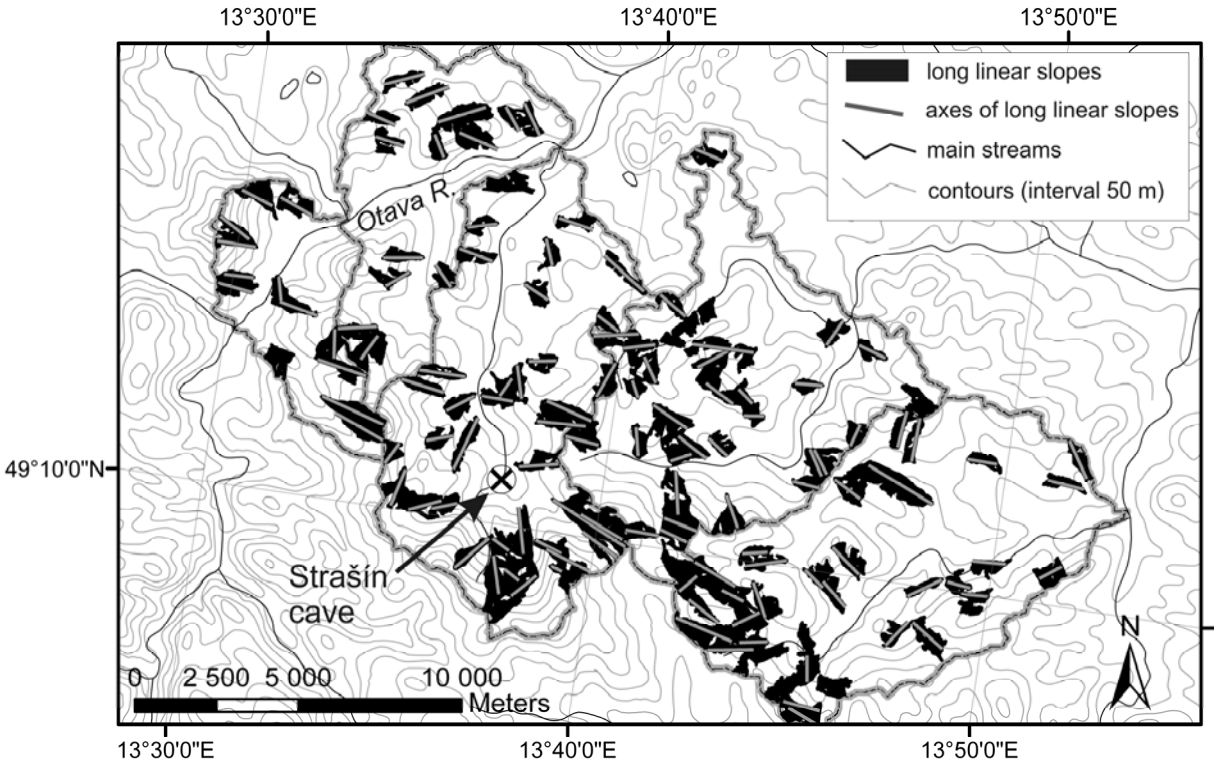


**Fig. 3** Map of the Area of Interest (AOI) used for morphostructural analysis showing the long linear slopes (LLS) and their axes used in the analysis.

This layer was evaluated in the analysis of the elongated slopes. The total length of the large linear slope axes was 133 km.

All the sets of linear features have been analysed using rosette diagrams. The data were grouped into intervals of azimuth by 10 degrees in the range 0-180. Each interval is centred on the decimal value, i.e. the interval labelled '10°' incorporated values between 6 and 15 degrees. To obtain comparable results, all the sets were then weighed by length and reclassified into percentages. The results of the morphological analyses have been displayed in summary rosette charts. These allow a direct comparison of the orientation of the linear datasets.

### *2.2. GEOPHYSICAL MEASUREMENTS*

In our research we have applied geophysical methods for the mapping of fault systems, the identification of marble blocks in the surrounding paragneiss, and in the search for cavities within these blocks. To solve these tasks we have used geoelectrical methods in the form of pole-dipole profiling, multielectrode resistivity, and gravimetry.

#### *2.2.1. RESISTIVITY PROFILING*

Resistivity profiling is a method used mainly for the mapping of conductive zones such as ore veins or fault zones. In our work, we have used a combination of forward and reversed pole-dipole electrode configurations and a DC source. This configuration is suitable even in areas with a complex geological structure (e.g. Valenta et al., 2008). The pole-dipole configuration is a three electrode configuration with the first current electrode A (or B in the reversed configuration) and the potential electrodes M and N on the profile, while the second current electrode C is in the "infinity" (e.g. Telford et al., 1990; Burger, 1992; Reynolds, 1997).

The electrode separation were configured in such a way (A40M10N40B) that the depth reach of the method was about 30 metres. This then eliminates near-surface inhomogeneities and emphasises large-scale structures. The pole-dipole profiling was carried out on nine profiles surrounding Strašín Cave (Fig. 4).

#### *2.2.2. MULTIELECTRODE RESISTIVITY METHOD*

The multielectrode resistivity method is an elaborate vision of resistivity profiling. It uses a large number (dozens) of electrodes on the surface and the automatic measuring unit switches them alternatively to be current or potential (Loke and Barker, 1996) and, hence, maps the distribution of resistivity with depth along the profile (in the 2D case).

In this method, we have used the dipole-dipole configuration of electrodes to get a highly detailed picture of the sub-surface. The electrode step on the surface was 4 metres and the maximal depth reach

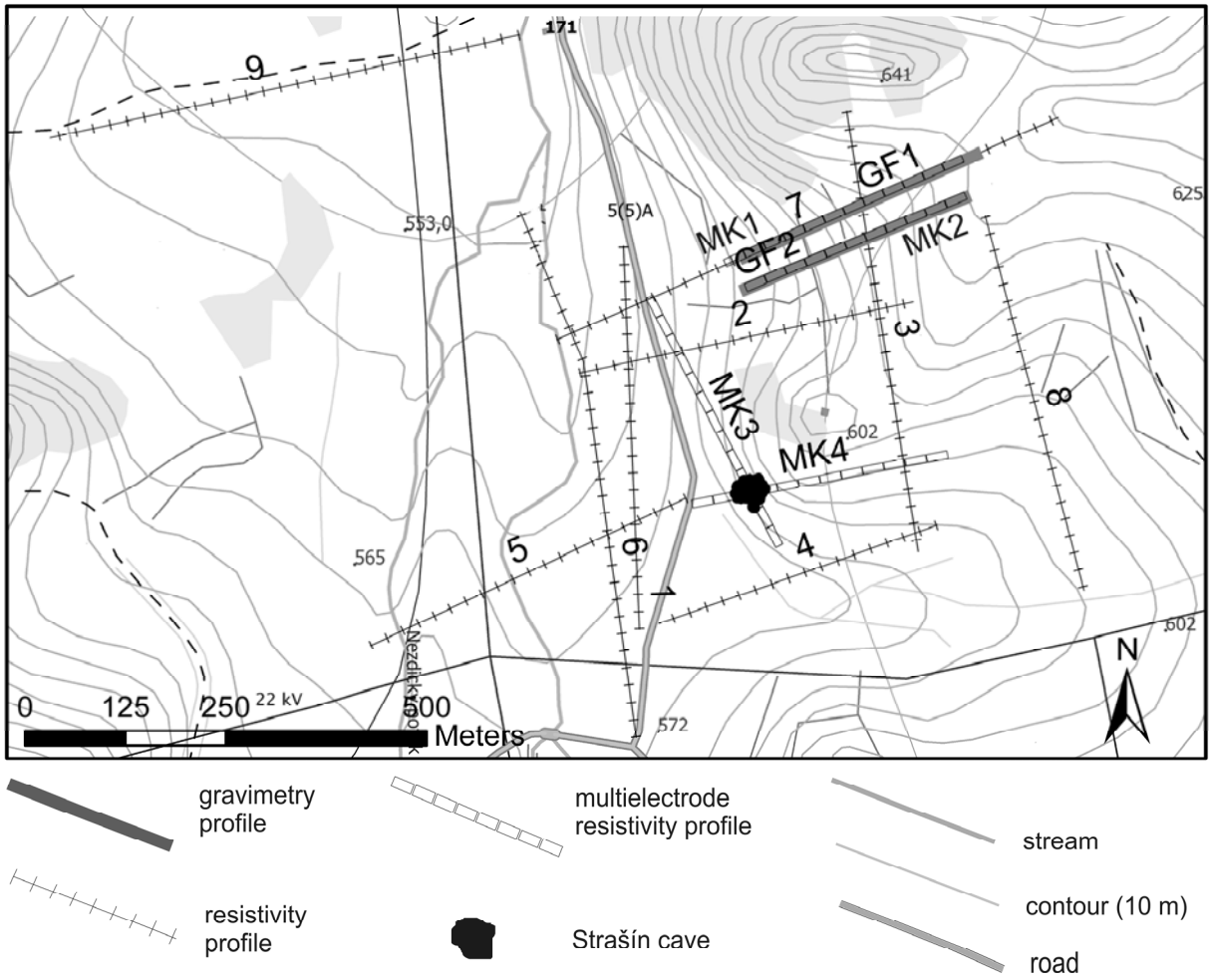


**Fig. 4** Map of the closest surroundings of the Strašín cave with the position of the geophysical profiles. GF 1-2 stands for gravity profiles, MK 1-4 for ERT profiles, RP are only numbered.

was about 80 metres. The dipole-dipole configuration was selected according to a preliminary forward modelling, where it showed the best results for supposed target structures and geological medium. Moreover, to achieve a high data coverage and quality we have used combination of several a-spacings and N-separations with overlapping data layers. The maximum N-separation used was 4. The multielectrode resistivity measurements were performed along four profiles (Fig. 4). One pair ran over Strašín Cave (Profiles 3 and 4) and the other pair were measured over a potential cave (Profiles 1 and 2).

*2.2.3. APPARENT RESISTIVITY MAPPING*

The apparent resistivity raster was calculated to observe the distribution of resistivity in the close vicinity of the cave. This helps to differentiate various underlying environments as well as to interpret the bedrock type, state, and character (Abu Shariah, 2009).

We have used a combination of the four-electrode Schlumberger array as an average value for the apparent resistivities measured by the forward and reversed pole-dipole. However, as the data in the area closest the cave were missing, we complemented them with adapted data retrieved from the inverted multielectrode resistivity profiles covering this area.

Here, the problem was two-fold. First, from the multi-layered ("multielectrode") output, we had to separate the layer, which would correspond to a depth range for the RP profiles. The depth range of the Schlumberger array is usually estimated to be one quarter of the current electrodes distance. Hence, in our case, for the electrode configuration A40M10N40B, the depth range is about 20 metres.

Second, was the fact that the observed resistivity pattern for the same anomaly differs substantially between the Schlumberger and dipole-dipole array. Hence, we had to combine measured resistivity curves from the Schlumberger array (apparent resistivities) with the inverted "true" resistivities from the dipole-

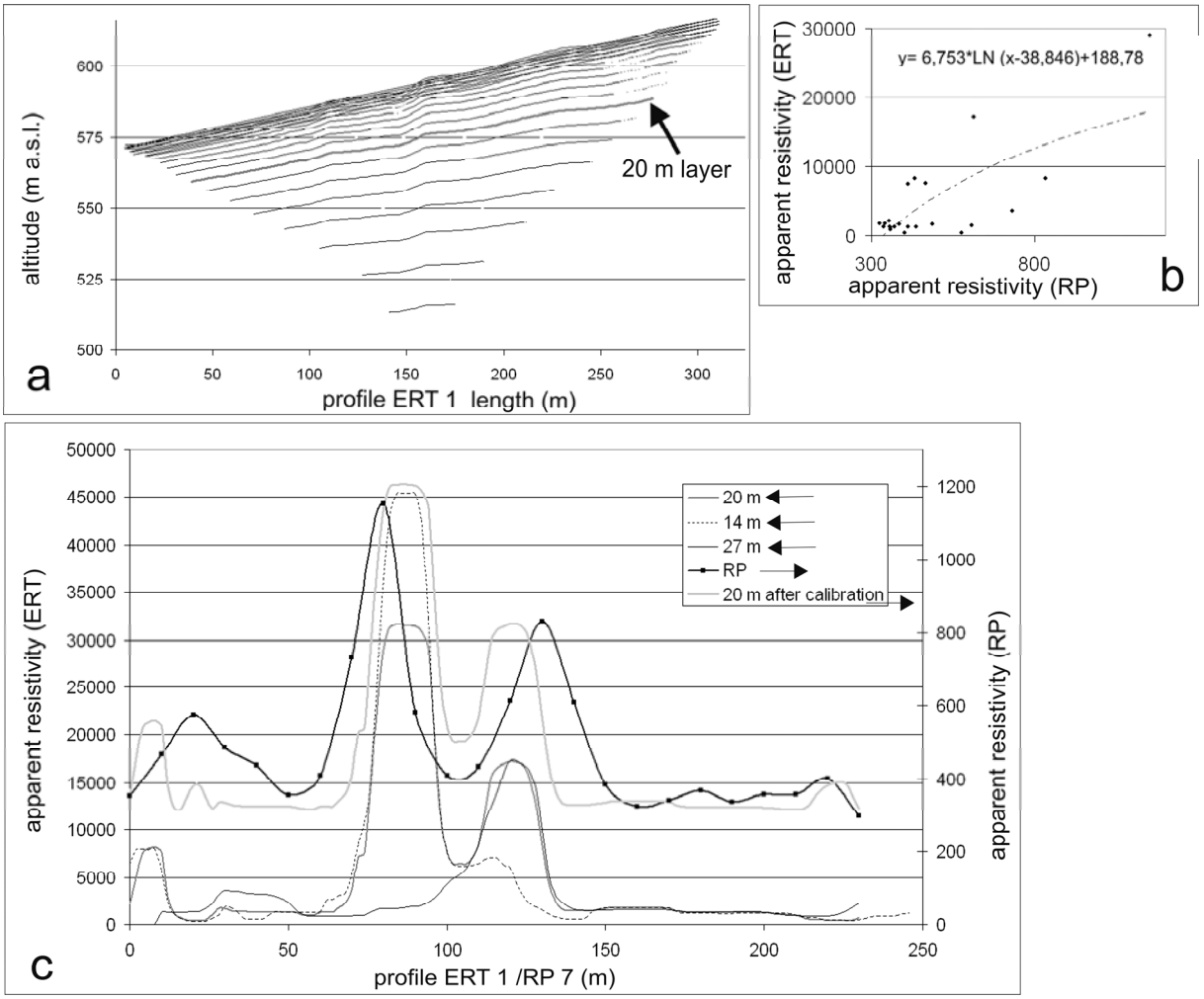


**Fig. 5** A set of charts illustrating the extraction of data from multielectrode profile and their conversion to correspond to the resistivity profiling values. a) ERT profile No. 1 showing the measured layers indicating the 20 m layer corresponding to the depth of RP in constellation A40M10N40B. b) Correlation between the apparent resistivity dataset of 20 m layer of ERT profile 1 with apparent resistivity of RP profile 7. c) A chart showing the apparent resistivity values of 20 m layer before and after calibration, compared with two neighbouring layers (14 and 27 m). Arrow in the legend indicates against which vertical axis the values are plotted.

dipole array. These are closer in their sense of shape but naturally differ in magnitude.

The calculation indicated that we should look for the layer at a depth of 20 m. This was confirmed by the resistivity curves comparing RP Profile 7 with multielectrode Profile 1. These were measured along the same profile line (Fig. 5).

Next, it was necessary to adjust the resistivity values, which naturally had different values. A regression curve was calculated, again using the data from RP Profile 7 and multielectrode Profile 1. The resulting regression formula was used for transforming the other three multielectrode profiles. The result was merged with the resistivity profile data.

Interpolation of multiple, irregular profile data is generally problematic (Sibson, 1981; Watson, 1992). In one specific direction (profile course), the data are dense and regular. In the other directions, the data are extremely irregular both in distance and direction. Therefore, instead of common kriging or IDW, we decided to use the natural neighbour method (also known as Sibson interpolation) as this works equally well with regularly and irregularly distributed data (Watson, 1992). Using Thiessen polygons, the interpolation deals only with the directly neighbouring points and does not "invent" extremes outside the interval of any given dataset. It also allows the use of sharp divisions (breaklines), useful for limiting expectedly different bodies.

As the next step, we computed the apparent resistivity values for the four-electrode Schlumberger array as an average value of the apparent resistivities

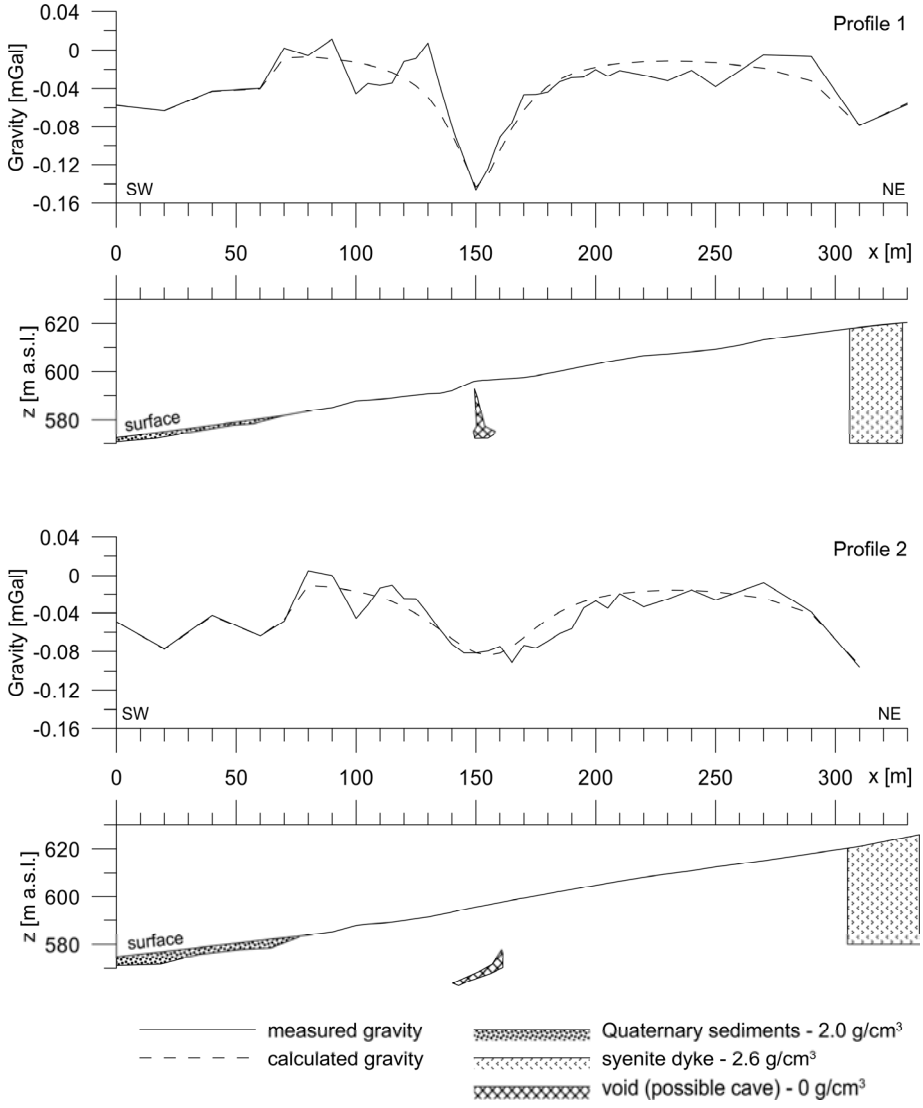


**Fig. 6** Gravimetry profiles located approx. 200 m N from the Strašín cave showing possible occurrence of another underground cavity. For each profile, upper chart is measured and modelled gravity, lower is the gravity material model.

measured by the forward and reversed pole-dipole. These "Schlumberger array" apparent resistivities have been gridded into the map.

The resulting map, however, lacked data in the central part around the cave. Therefore, we used the multielectrode Profiles 2, 3, and 4 as a source of data for this space. Using the embedding technique described previously, we included the multielectrode data in the raster interpolation. The recalculated layers were used as another input for the interpolation of the apparent resistivity grid.

*2.2.3. GRAVITY SURVEY*

Gravity survey is a method for mapping changes in rock density. The gravity meters used for prospecting measure the relative gravitational acceleration along a profile or survey grid (Mochales et al., 2008). The changes in acceleration correspond to changes in rock density (Boler, 1984). The usual targets for gravity survey are salt domes, voids, and large-scale geological mapping. It is known that the possible cave would reveal itself as an area with a mass deficiency (Boler, 1984; Mochales et al., 2008) and, therefore, with decreased gravitational acceleration.

To obtain a gravity value on individual points we have used several 60 seconds long measurements on the same place to get three consistent gravity readings without outliers. Next, the average of these three readings was used as a gravity reading for further processing.

The second step in the data processing was the drift correction based on repeated readings on the base station within the measured area. The tidal correction

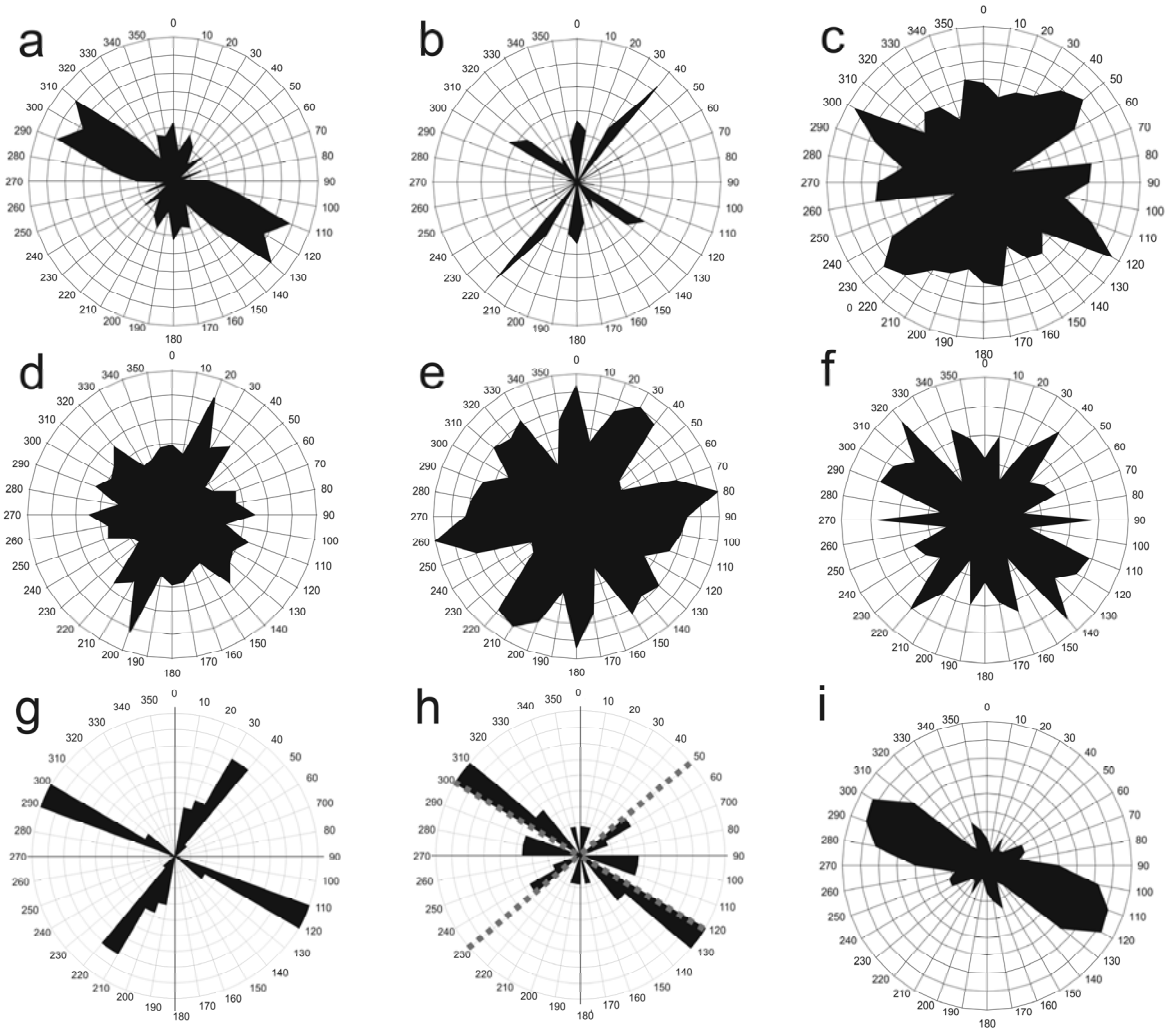


**Fig. 7** Stiny rosette diagrams showing the directions of morphostructural and morphological elements of the relief. All the diagrams are relativised. a) morpholineaments from 10 m raster (whole AOI), b) morpholineaments based on 100 m DEM, c) stream segments (100 m), d) thalwegs, e) thalwegs (western part), f) thalwegs (eastern part), g) faults from the 1:50 000 geological map, h) joints inside the cave (grey dotted lines indicate the direction of monitored faults inside the cave), i) large linear slopes axes (LLS).

is automatically computed by the gravity meter and its possible uncompensated residual is removed within the drift correction.

The third step was calculation of the free-air and Bouguer corrections (e.g. Blafly, 1996). The estimation of a reduction density for the Bouguer correction was based on the Nettleton's method (Nettleton, 1939) and found to be 2.7 g/cm$^3$.

The last step in the data processing was removing the regional (linear) trend from the data to emphasise the effects of small-scale local structures. The regional trend was estimated from the data on the flanks of the profiles not affected by the gravity effect of the possible cave.

Gravity measurements have been undertaken on two parallel profiles above the possible cave (Fig. 6). These two profiles have been taken along multielectrode resistivity Profiles 1 and 2. The measured gravity data were processed into Bouguer anomalies, with an applied reduction density of 2.7 g/cm$^3$). The regional (linear) trend was then removed. The final residual gravity data exhibit a distinct gravity low about the *x*-coordinate 150 m (Fig. 11), where the possible cave was expected.

## 3. RESULTS

### *3.1. STRUCTURAL AND MORPHOLOGICAL RESEARCH*

The first lineament set, derived from the 10 m DEM (Fig. 7a), comprise a total 920 km of morpholineaments. The second set, derived from 100 m DEM, comprise a total 79 km of morpholineaments (Fig. 7b). All the 168 lineaments considered in the first set were longer than 300 m, with a mean length of 1.4 km and a maximum length of over 5 km. The 24 lineaments considered in the

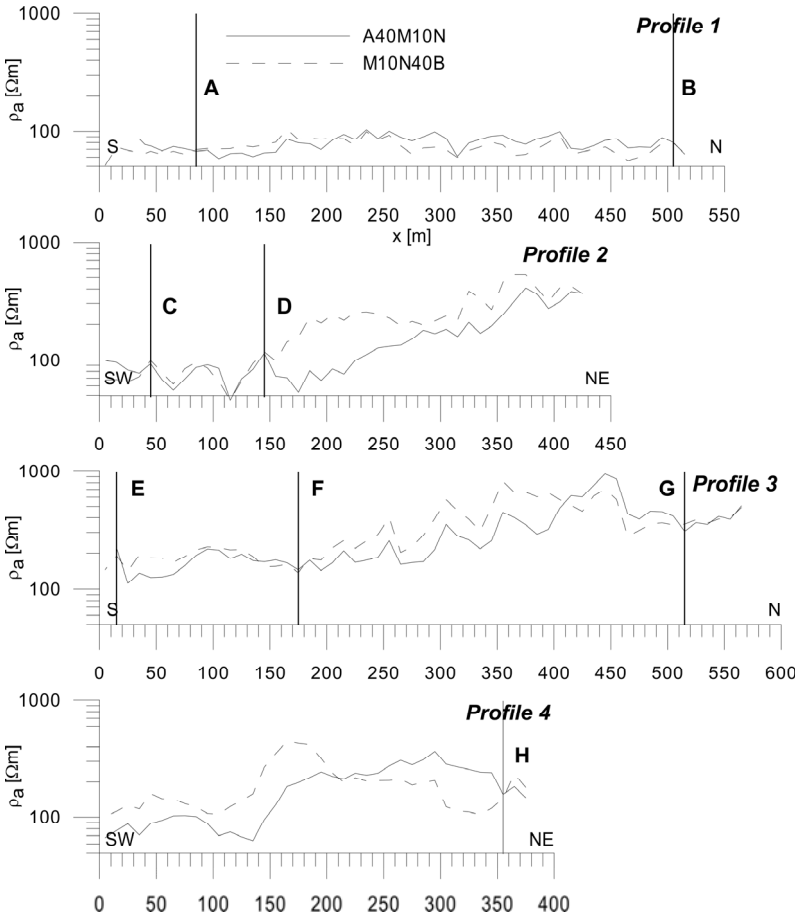


**Fig. 8a** Charts of apparent resistivity of the resistivity profiling around Strašín cave. Lettered lines represent indications of an electric conductor (a fault zone). For position of the profiles see Figure 4 - First RP campaign (profiles 1-4),

second set had a mean length of 3.3 km and ranged from 1.5 to 7 km.

The directions of the stream segments were obscured by fine segmentation (Fig. 7c). Nevertheless, the main features remain observable. The most frequent stream segment directions are approximately NW-SE (~ 120°), NE-SW (40°- 60°), and SSE-NNW (~ 170°). However, slightly more robust results were derived from the analysis of thalwegs (Fig. 7d). The simplified drainage network shows more clearly preferred stream orientations, particularly when the area of interest was split into eastern and western sections. In the eastern part (Fig. 7e), practically all the regional tectonic directions found in Pošumaví (Hartvich, 2004) are present. The more prominent directions are WNW-ESE and N-S, followed by 30°- 40° and the roughly perpendicular 130° - 150°. In the western part (Fig. 7f), the most frequent directions are NE-SW (30°- 40°) and NW-SE (110° - 140°).

As only a few faults are depicted on the 1:50 000 geological map, the rosette is simple (Fig. 7g). The only significant systems are oriented to the direction of 20°- 40° and its perpendicular counterpart 110°- 120°. The faults closest to the cave also follow these directions. Measurements of tectonic joints inside the cave were complicated by the scarcity of measurable structures due to the fact that many of the joints have been eroded to form parts of the cave itself. Nonetheless, the most common joint directions are 120°- 130°, 50°- 60°, 90°- 110 (Fig. 7h). Two devices measure active displacements in the cave, one on a 120°- 130° joint and the other on a 50°- 60° joint.

The axes of the large linear slopes are most commonly oriented from WNW-ESE to NW-SE (Fig. 7i). This corroborates the fault and lineament orientations and the general inclination of the study area to the NNE-NE. Two secondary directions can also be observed: 60°- 70° and ~ 160°.

To summarise the morphostructural results, we can state that the area of interest is strongly influenced by tectonic structures that have originated during various tectonic regimes. This is illustrated by the similarity of orientation of relief elements with the structural lineaments. While the most common linear

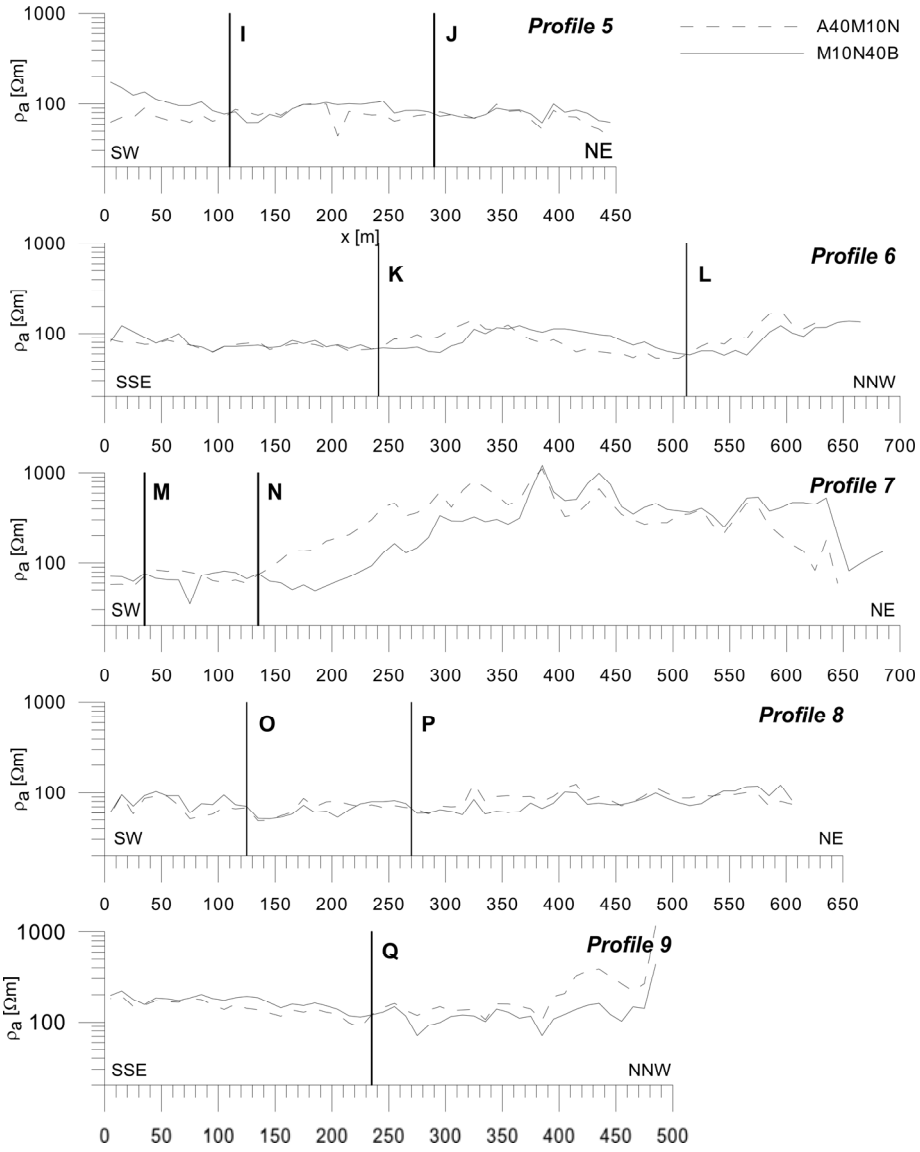


**Fig. 8b** Charts of apparent resistivity of the resistivity profiling around Strašín cave. Lettered lines represent indications of an electric conductor (a fault zone). For position of the profiles see Fig. 4 - Second RP campaign (profiles 5-9).

segment orientation oscillates generally around NW-SE (or slightly turned towards the east, 110°- 130°; the Šumava direction) (Figs. 7a, i), perpendicular directions occur as well; these most commonly oscillate between 20°- 40° (Figs. 7d, e). Less abundant orientations, observable particularly in the northwestern part of the study area, include N-S (or slightly NNW-SSE) and the more scarce 60°- 70°.

### *3.2. GEOPHYSICS*

#### *3.2.1. RESISTIVITY PROFILING*

The measured data obtained by resistivity profiling were processed in two different ways. The first was to look for conductive zones based on "crossings" of forward (AMN) and reversed (MNB) pole-dipole resistivity curves. Some of these conductive zones could represent fault zones (Figs. 8a and b: marked A-Q). Each profile contained at least one such conductive zone.

#### *3.2.2. MULTIELECTRODE RESISTIVITY METHOD*

The multielectrode resistivity method was measured on four profiles. Two crossed the high-resistivity zone discovered by the resistivity profiling. The other two ran across Strašín Cave (Fig. 4). This enabled a direct comparison of results. The inter-electrode distances on the profiles were four metres and the electrode configuration for measurements was dipole-dipole. Measured apparent resistivities were inverted using the software Res2dInv by M. H. Loke (Loke and Barker, 1996) in order to get the true depths and resistivities of geological structures. We have

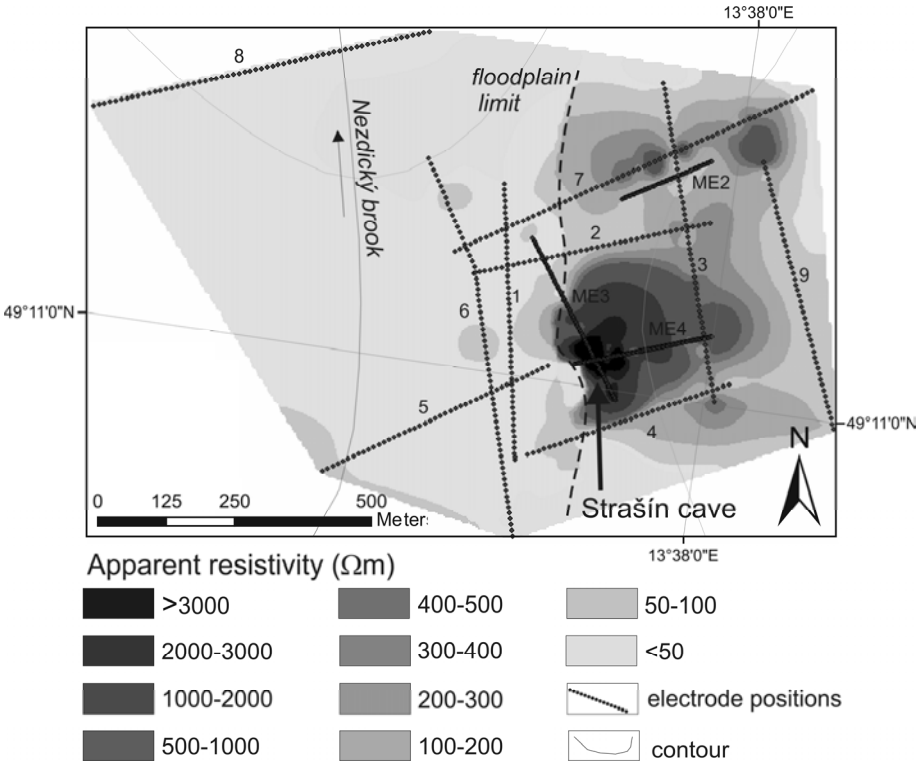


**Fig. 10** Map of apparent resistivity calculated from the RP profiles 1-9 and from the ERT profiles 2-4.

used the $l_2$-norm (robust) inversion method and the Jacobian matrix was recalculated at every inversion. The inverted profiles are shown in Figures 9a-d.

Profile 1 (Fig. 9a) crosses two high-resistivity areas, most likely marble blocks. The first is located between the *x*-coordinates 40-100 m. The second is shallower, about 20 metres thick, and lies between the *x*-coordinates 100-160 m. According to the gravimetry (see the next section), this area of high resistivity most likely comprises a cave.

Profile 2 (Fig. 9b) was positioned 40 m southwest and parallel with Profile 1. It reveals the two high-resistivity anomalies already found on the previous profile. However, the anomaly with a possible cave is wider here (*x*-coordinates 140-160 m) and continues to a greater depth.

Profile 3 crosses the marble block of Strašín Cave between *x*-coordinates 40-110 m. The values of resistivity within this block are close to those on Profile 1. According to the values of resistivity on this profile, two groups of rock can be distinguished. The first group is represented by a high-resistivity area (> 600 Ωm) and is most likely composed by marbles. Three possible marble blocks can be distinguished here. The second group is represented by low resistivities (< 200 Ωm). This group probably consists of paragneiss affected to various degree by the weathering. Three indications of faults were distinguished at 40 m, around 170 m and at 300 m.

Profile 4 crosses the marble block of Strašín Cave between *x*-coordinates 50-130 m. The resistivity image on this profile is not as clear as that on Profile 3. It seems that even resistivity values of about 1000 Ωm could represent paragneiss. However, these would then be only slightly weathered and possibly contain large amount of quartz. An indication of fault was identified around 170 m.

Generally, we can state that the known cave on profiles 3 and 4 is marked with similarly high resistivity values as the gravity anomalies´ surroundings on profiles 1 and 2. The marbles, in which has developed the Strašín cave, are typically more resistant than neighbouring weathered, fault-containing gneisses.

### *3.2.3. APPARENT RESISTIVITY MAPPING*

The map of apparent resistivities (Fig. 10) depicts clearly two distinct areas: a low-resistivity and a high-resistivity area. The low resistivity area is situated on the eastern side of the locality and is characterised by apparent resistivities of about 100 Ωm or less. The low apparent resistivities are caused by saturated clayey and silty-sandy Quaternary fluvial and alluvial sediments, which are probably several metres thick.

The high-resistivity zone is located on the western side and is characterised by apparent resistivities of about 220 Ωm or more. The high values

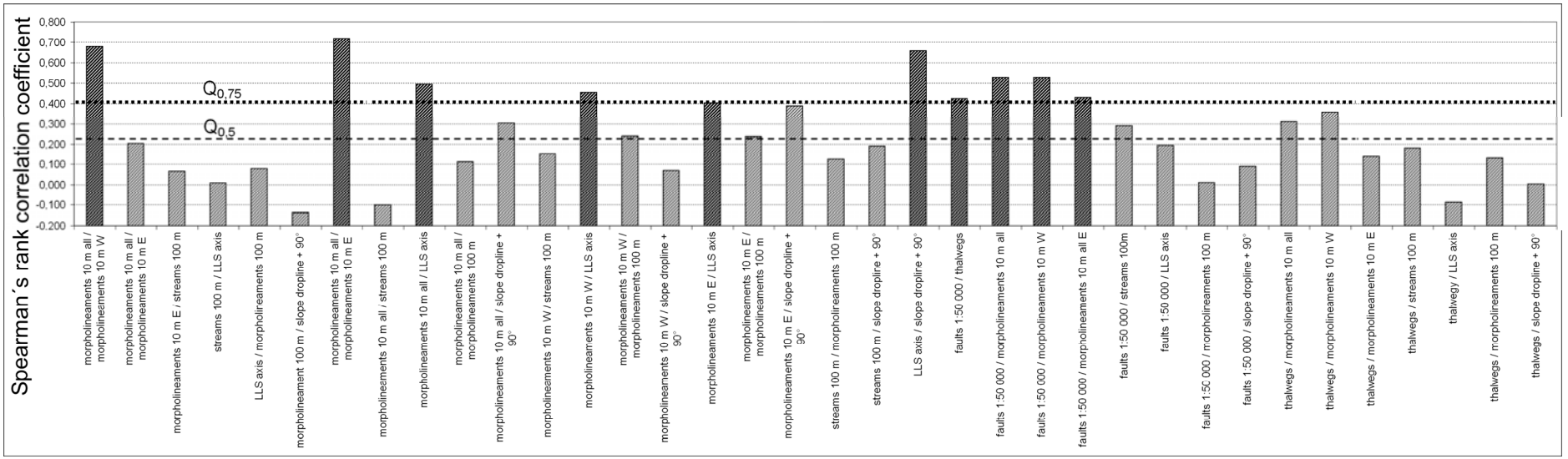


**Fig. 11** Bar chart showing the values of Spearman's rank correlation coefficient for each pair of morphostructural elements. Darker hatching have the pairs with coefficient values above $Q_{0,75}$ (0,42), which may be considered to correlate significantly.

of apparent resistivities reflect the presence of paragneiss, marble blocks, and several dykes of erlan (lime silicate rock) and syenite. The highest values of apparent resistivities within this zone (more than 500 Ωm) crossed by Profiles 3 and 7 is most likely caused by the presence of a marble block with a possible cave. Since it is not possible to prove or reject the presence of a cave from resistivity profiling, the area has been further investigated using the multielectrode resistivity method and gravimetry.

#### *3.2.4. GRAVIMETRY*

A simple 2.5D density model has been constructed (Fig. 6). This consists of a paragneiss and marble background (density 2.7 g/cm$^3$, the same as that used for the Bouguer slab), Quaternary sediments (density 2.0 g/cm$^3$), a syenite dyke (density 2.6 g/cm$^3$), and a possible cave (density 0 g/cm$^3$). For the forward numerical computations, we have used the software Geomodel (Cooper, 2010).

After series of model optimization, we have obtained a good fit between the measured and computed gravity. These data together with the final model can be found in Figure 6. On both profiles, we can observe the void space approximately around 150 m and 10-20 m deep. This coincides with the location of the anomalies on both simple and ERT resistivity profiling.

## 4. DISCUSSION

Although the village of Strašín is close to the mining region of Kašperské Hory, no detailed geomorphological or geological research has been carried out (or, at least, published) in this area. The only exceptions are the geological mapping carried out by the Czech Geological Survey (Babůrek, 2001; Babůrek et al., 2001) and a few older specialized studies such as a report on limonite crusts in Strašín Cave (Kukla and Skřivánek, 1954) or research on the Pošumavský Karst (e.g. Kunský, 1930; Prosová, 1950).

### *4.1. MORPHOSTRUCTURAL ANALYSIS*

In a situation where suitable outcrops for microtectonic measurements do not occur, relief morphology offers an alternative source of morphostructural information (Jordan et al., 2005; Štěpančíková, 2007).

The geological literature concerning the tectonic properties of the study area is rather sparse. However, the general structural directions identified here are in agreement with previously recorded observations. Rather surprisingly, lineament directions clearly show a morphostructural difference between the eastern and western parts of the study area. This can be explained by dividing the area of interest into two different morphostructures (sensu Fiala, 2005). Moreover, this division corresponds to the geological sub-division with the Uniform Series to the east and the Varied Series to the west (Mísař et al., 1983).

The direction of faults, morpholineaments, thalwegs, and slope axes were compared visually, using rosette diagrams, and statistically, using Spearman's rank correlation coefficient. In total, 36 pairs combined from 9 datasets were compared (Table 1 and Fig. 11).

The best correlation could be observed between the morpholineaments from the 10 m raster, long linear slope axes, and faults (if we leave aside the correlation with eastern and western subsets). This clearly indicates the strong and persistent influence of tectonics on the current relief (Jordan et al., 2005), similarly as was described by Mentlík et al. (2010), who analysed links between tectonic predispositions and current form of the glacial cirques in the upper parts of the Bohemian Forest Mts. More problematic is the correlation of stream segments, which are blurred by meandering, and of lineaments based on the coarser raster (100 m), which are too few in the study area.

The joint directions measured in the cave by the authors and by Kukla and Skřivánek (1954) are shown in Figure 7k The most frequent direction is 120°- 130° (monitored in the cave by device 1), followed by 50°-60° (monitored in the cave by device 2), and 90°-110°. As a comparison, Kukla and Skřivánek (1954) describe joint directions of 135°, 70°, and 120°.

The closest roughly corresponding NE-SW faults on the 1:50 000 geological map have directions of 35°- 40° while the fault monitored by device 1 has a direction of 60°. However, Babůrek et al. (2001) included on the 1:25 000 map yet more faults. In particular, a NNW-SSE fault (the Kvilda direction) predisposes the valley of Zuklínský stream and several parallel SW-NE faults, observable in a nearby quarry, predisposes the valley of Nezdický stream.

### *4.2. GEOPHYSICAL MEASUREMENTS*

Combining the results of the geophysical survey with the results of the morphostructural analysis formed the principle aim of this paper. It is necessary to connect the conductor indications in the resistivity profiles with the joint system and measured faults inside the cave and to analyse the known fault structures nearby to see if they represent continuations of the identified structures.

The best fit between the faults observed inside the cave is shown in Figure 12. The fault on which device 1 is located has an approximate direction of 60°. This corresponds to one of the main directions observed in the surrounding relief (i.e. in the long linear slopes axes, valley segments) and roughly also to the perpendicular fault direction (see above). The nearest fault described by Babůrek et al. (2001) to the cave, as well as the fault observed by Pelc and Šebesta (1994) approximately 1 km southeast of the cave, follow the same direction. This course corresponds to a line of conductivity anomalies A, F, and K (Profiles 1, 3, and 6, respectively).

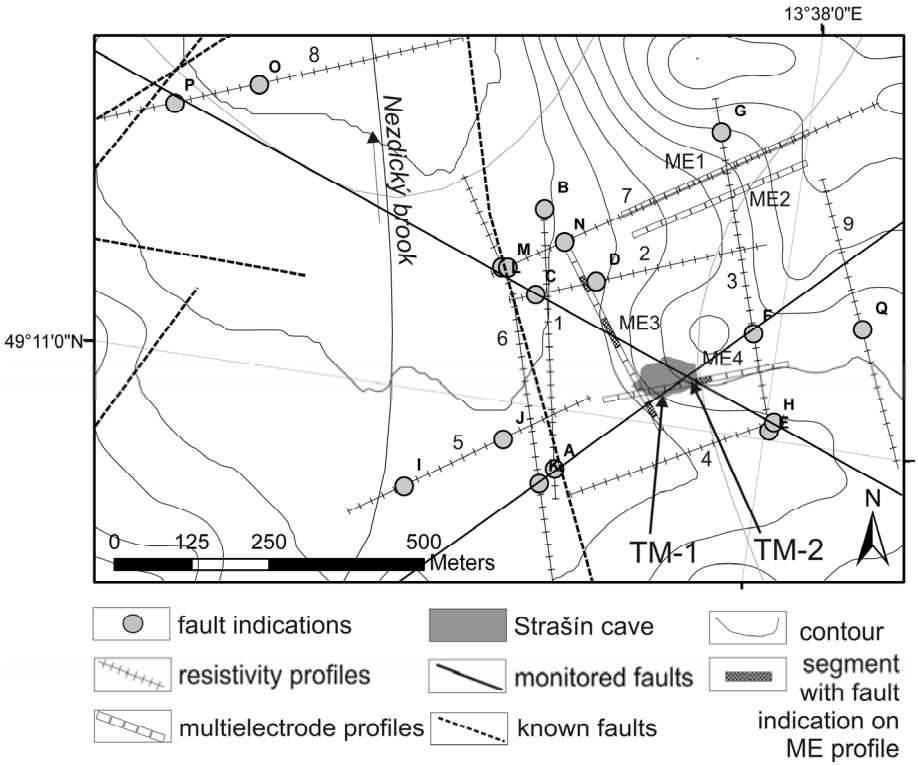


**Fig. 12** Map of the interpreted tectonic situation in the close vicinity of the Strašín cave. ME (multielectrode) stands for ERT profiles, RP are only numbered.

The fault on which device 2 is located has an approximate direction of 120°. This fault can be seen in anomalies F and H (Profiles 3 and 4) and in the northwest direction by anomalies C (Profile 3), L (Profile 6), M (Profile 7), and P (Profile 8).

In addition, we have tried to interpret the gravity and multi-cable results in the area northeast of the cave. The position of a distinct gravity low around *x*-coordinate 150 corresponds, according Kukla and Skřivánek (1954), to a site marked by a conic depression (possibly a sinkhole?) later filled by farmers. This could explain the cavern beneath as it may relate to a sinkhole.

We have modelled the cave on *x*-coordinate 150 of both gravimetric profiles, where the distinct isolated gravity low and high resistivity anomalies were observed. This cave is not filled with sediments and has not been discovered before. The depth of the cave is about 23 metres and is of highly irregular shape. The interpreted height varies between 3 and 7 metres and its maximum width is about 20 metres. The position of modelled cave fits well with the high-resistivity anomaly found on the multielectrode profiles.

The gravity low on the southwest of both profiles is interpreted as an increase in the thickness of the Quaternary sediments, as it corresponds to the very low resistivities found in this area on the multielectrode profiles.

The gravity low found on the northwestern side of both profiles is beyond the range of the multielectrode survey and, in accord with the geological map of Babůrek (2001), is interpreted as a syenite dyke. The interpreted width of the dyke (20–30 meters) corresponds well with that suggested by Babůrek et al. (2001). Furthermore, the interpreted density (2.6 g/cm$^3$) fits well within the usual bounds for syenite and nepheline-syenite (e.g. Jacoby and Smilde 2010).

The multielectrode results have enabled us to also estimate the size of the marble blocks. In the first approximation, it can be considered that the areas with resistivities of several thousands Ωm are composed of marble. This implies that the size of the marble block in which the newly discovered cave is located (Profile 1, *x*-coordinates 100-160) is roughly the size as the one in which Strašín Cave is located (Profiles 3 and 4, *x*-coordinates 40–110). Moreover, there is probably another large marble block on the southwestern side of Profiles 1 and 2 which is slightly deeper than the first one. From the results of Profile 2, it appears that both marble blocks could be connected. This hypothesis is also supported by the interpreted shape of the cave, which is elongated and dips in the direction of the larger deeper block on Profile 2. This leads to the hypothesis that the new cave could be much larger than Strašín Cave.

## 5. CONCLUSIONS

We have presented the results of an extensive morphostructural and geophysical study around Strašín Cave. This study was motivated by the need to link the faults monitored inside the cave to the regional tectonic system in the Pošumaví. From the morphostructural results, it is clear that the study area is strongly affected by tectonic structures developed through its long and complex geological history. These structural elements are, however, obscured by geomorphological processes. Therefore, the structural influence is not always readily identified and may only be revealed in, for example, the orientation of the stream network or slopes. From the dense network of resistivity profiles, an apparent resistivity map has been constructed in the vicinity of the cave.

The combination of morphostructural and geophysical research around the cave has demonstrated the suitability of the methodology for the declared purpose of the research, i.e. linking the monitored faults with tectonic structures in the vicinity of the cave. This has demonstrated two things. First, it is possible to link faults inside and outside the cave. This can done where the relevant faults are not found on surficial outcrops or even where surficial outcrops do not occur. Second, the measured faults are unlikely to be small cracks or minor discontinuities limited to the massif closest to the cave. Therefore, we may expect accurate and relevant results from microtectonic displacement monitoring. An unexpected finding has been derived from the geophysical survey. A combination of resistivity profiling and gravimetry has indicated the presence of a vault space about 20 m below the surface approximately 200 m northeast of Strašín Cave.

## ACKNOWLEDGEMENTS

The authors gratefully acknowledge financial support of the Institutional Research Plan AVOZ30460519 and Project No. B300460803 of the Grant Agency of the Academy of Sciences. The authors would like to thank Dr. Matt Rowberry for editing this paper. We would also like to thank Dr. Pavel Mentlík and an anonymous reviewer, who contributed to improvement of the paper by reviewing the text and giving us feedback with constructive and useful remarks. Finally, the authors express their thanks to the colleagues who helped them with the field measurements.

## REFERENCES

Abu Shariah, M.M.I.: 2009, Determination of cave geometry by using a geoelectrical resistivity inverse model. Engineering Geology 105, 239–244.

Babůrek, J.: 2001, Geological map of CR 1: 25 000, sheet 22-332 Kašperské Hory. Czech Geological Survey, Prague.

Babůrek, J., Fürich, V., Goliáš, V., Hanžl, P., Kadlecová, R., Lhotský, P., Nekovařík, Č., Nývlt, D., Osterrothová, K., Pertoldová, J., Strnad, L., Šebesta, J. and Vlčková, L.: 2001, Legend to the geological map of CR 1:25 000, sheet 22-332 Kašperské Hory. Czech Geological Survey, Prague.

Babůrek, J. et al.: 2006, Geologie Šumavy. Šumava National Park Authority, Vimperk.

Balatka, B. and Kalvoda, J.: 2005, Geomorfologické členění reliéfů Čech (Geomorphological regionalization of the relief of the Czech Republic).Kartografia a.s., Praha, 79 pp., (in Czech).

Blakely, R.J.: 1996, Potential theory in gravity and magnetic applications. Cambridge University Press, Cambridge.

Briestenský, M., Košťák, B., Stemberk, J., Petro, L., Vozár, J. and Fojtíková, L.: 2010, Active tectonic fault microdisplacement analyses: a comparison of results from surface and underground monitoring in western Slovakia. Acta Geodyn. Geomater., 7, No. 4 (160), 387–397.

Burger, H.,R.: 1992, Exploration Geophysics of the Shallow Subsurface, Prentice Hall P T R, New Jersey.

Butler, D.K.: 1984, Microgravimetric and gravity gradient techniques for detection of subsurface cavities: Geophysics, 49, 1084–96.

Casas, A.M, Cortes, A.L, Maestro, A., Soriano, M.A., Riaguas, A. and Bernal, J.: 2000, LINDENS: A program for lineament length and density analysis. Computers & Geosciences. 26, Issues 9-10, 1 November 2000, Pages 1011–1022

Clark, C.D. and Wilson, C.: 1994, Spatial analysis of lineaments. Computers and Geosciences, 20, No. 7/8, 1237–1258

Cooper, G.R.J.: 2010, Geomodel – 2.5D Simultaneous magnetics and gravity modelling and inversion, Version 2.01. Johannesburg, University of the Witwatersrand. http://web.wits.ac.za/Academic/Science/GeoSciences/Research/Geophysics/GordonCooper/Software.htm, visited December 28th 2010.

Čech, V. et al.: 1962, The legend to the general geological map of the Czechoslovakia 1:200 000, sheets České Budějovice and Vyšší Brod. Geofond, Prague, 192 pp.

Ekneligoda, T.C. and Henkel, H.: 2010, Interactive spatial analysis of lineaments. Computers & Geosciences. 36, Issue 8, August 2010, Pages 1081–1090

Fiala, T.: 2005, Pojetí morfostrukturní analýzy reliéfu v pracech českých a slovenských geomorfologů. (Morphostructural analysis in the works of Czech and Slovak geomorphologists). Geografie – Sborník ČGS, 110, 2, 103–115.

Guerin, R., Baltassat, J.-M., Boucher, M., Chalikakis, K., Galibert, P.-Y., Girard, J.-F., Plagnes, V. and Valois, R.: 2009, Geophysical characterisation of karstic networks – Application to the Ouysse system (Poumeyssen, France). Comptes Rendus Geosciences. 341, Issues 10-11, October-November 2009, Pages 810–817.

Hartvich, F.: 2004, Morfostrukturní analýza sv. okraje Šumavy v okolí Pošumavského zlomu (Morphostructural analysis of the NE margin of the Bohemian Forest Mts. in the vicinity of the Pošumavský fault). Proceeding of the workshop "State of gomorphological and Quaternary-geological research in the Bohemian Forest Mts. in 2004, Miscellanea Geographica 10, ZČU, Plzeň, 2004, 115–127.

Hartvich, F. and Valenta, J.: 2011, Combining the geophysical and morphostructural approach in the

research of an intra-montane tectonic fault. Under review, Acta Geodyn. Geomater., 8, No. 4 (164), 427–443 .

Jacoby, W. and Smilde, P.L.: 2010, Gravity Interpretation, Springer-Verlag, Berlin, Heidelberg.

Jordan, G., Meijninger, B.M.L., van Hinsbergen, D.J.J., Meulenkamp, J.E. and van Dijk, P.M.: 2005, Extraction of morphotectonic features from DEMs: Development and applications for study areas in Hungary and NW Greece. International Journal of Applied Earth Observation and Geoinformation, Volume 7, Issue 3, November 2005, 163–182.

Jordan, G. and Schott, B.: 2005, Application of wavelet analysis to the study of spatial pattern of morphotectonic lineaments in digital terrain models. A case study. Remote Sensing of Environment 94, 31–38.

Koike, K., Nagano, S. and Kawaba, K.: 1998, Construction and analysis of interpreted fracture planes through combination of satellite-image derived lineaments and digital elevation model data Computers & Geosciences.. 24, No. 6, 573–583

Křížek, M., Hartvich, F., Chuman, T., Šefrna, L., Šobr, M. and Zádorová, T.: 2006, Floodplain and its delimitation. Geografie – Sborník ČGS, 111, č.3., 314–325.

Kukla, J. and Skřivánek, F.: 1954, Limonitická výplň jeskyně u Strašína na Sušicku (Limonite fillings in the Strašín cave near Sušice). Věstník ÚÚG, roč. XXX, 113–126.

Kunský, J.: 1930, Primární krasové fenomeny v krystalickém vápenci u Strašína jv. od Sušice (Primary karst phenomena in crystalline limestone at Strašín near Sušice).Časopis Nár. Muzea, ročník CIV, Praha.

Loke, M.H. and Barker R.D.: 1996, Rapid least-squares inversion of apparent resistivity pseudosections using a quasi-Newton method. Geophys Prospect, 44, 131–152.

Mentlík, P., Minár, J., Břízová, E., Lisá, L., Tábořík, P., and Stacke, V.: 2010, Glaciation in the surroundings of Prášilské Lake (Bohemian Forest, Czech Republic) Geomorphology 117, 181–194.

Minár, J., Bielik, M, Kováč, M., Plašienka, D., Barka, I., Stankoviansky, M. and Zeyenet, H.: 2010, New morphostructural subdivision of the Western Carpathians: An approach integrating geodynamics into targeted morphometric analysis. Tectonophysics, in press, doi:10.1016/j.tecto.2010.04.003

Mísař, Z. at al.: 1983, Geologie Československa I (Český masiv (Geology of Czechoslovakia I - Bohemian massif). SPN, Praha, 336 pp.

Mochales, T., Casas, A.M., Pueyo, E.L., Pueyo, O., Roman, M.T., Pocovi, A., Soriano, M.A., and Anson, D.: 2008, Detection of underground cavities by combining gravity, magnetic and ground penetrating radar survey: A case study from the Zaragoza area, NE Spain: EnvironmentalGeology, 53, 1067–1077.

Müller, V., Burda, J., Kadlecová, R., Majer, V., Manová, M., Mrázek, P., Pelc, Z., Pošmourný, K. , Rejchrt, M. , Šalanský, K. , Šebesta, J. , Tojšl, P. and Tomášek, M.: 1999, Vysvětlivky k souboru geologických a ekologických účelových map přírodních zdrojů v měřítku 1:50 000 list 22-33 Kašperské Hory a 32-11 Kvilda (Legend to the set of geological and ecological thematic maps of natural resources in the scale 1:50 000 sheet 22-33 Kašperské Hory a 32-11 Kvilda). Český geologický ústav. Praha, 62 pp

Nettleton, L.L.: 1939, Determination of density for reduction of gravimeter observations. Geophysics, 4, 176–183.

Pánek, T., Margielewski, W., Tábořík, P., Urban, J., Hradecký, J. and Szura, C.: 2010, Gravitationally induced caves and other discontinuities detected by 2D electrical resistivity tomography: Case studies from the Polish Flysch Carpathians. Geomorphology 123, 165–180.

Pelc, Z. and Šebesta, J.: 1994, Geologická mapa 1:50 000, list 22-33 Kašperské Hory (Geological map 1:50 000, sheet 22-33 Kašperské Hory). GÚ, Praha.

Prosová, M.: 1950, K charakteristice krasu v krystalických vápencích jižních Čech (On the character of the karst in crystalline limestones in southern Bohemia). Sborník Čs. společnosti zeměpisné, roč. 1950, 196–203.

Raghavan, V., Masumoto, S., Koike, K. and Nagano, S.: 1995, Automatic lineament extraction from digital images using a segment tracing and rotation trarnsformation approach. Computers & Geosciences, 21, No. 4, 555–591.

Reynolds, J.M.: 1997 An Introduction to Applied and Environmental Geophysics, Wiley, New Jersey.

Sibson, R.: 1981, A brief description of natural neighbour interpolation. Interpolating multivariate data, John Wiley and sons, New York, 21–36.

Schrott, L., and Sass, O.: 2008, Application of field geophysics in geomorphology: Advances and limitations exemplified by case studies. Geomorphology, 3, Issues 1–2, 55–73

Skácelová, Z., Rapprich, V., Valenta, J., Hartvich, F., Šrámek, J., Radoň, M., Gaždová, R., Nováková, L., Kolínský, P. and Pécskay, Z.: 2010, Geophysical research on structure of partly eroded maar volcanoes: Miocene Hnojnice and Oligocene Rychnov volcanoes (northern czech Republic). Journal of Geosciences, 55, 299–311. doi: 10.3190/jgeosci.072

Stemberk, J. and Hartvich, F.: 2011,: Fault slips recorded in the Strašín Cave (SW Bohemian Massif). Acta Geodyn. Geomater., 4, No. 4 (164), 415–425.

Stemberk J., Košťák B. and Vilímek V.: 2003, 3-D monitoring of active tectonic structures, Journal of Geodynamics, 36, 103-112, Elsevier , London.

Štěpančíková, P.: 2007, Morfostrukturní vývoj severovýchodní části Rychlebských hor. (Morphostructural development of the north-eastern part of the Rychlebské Mts.). MS, KFGG PřF UK, Prague, 192 pp.

Telford, W., M., Geldart, L.,P. and Sheriff, R.E.: 1990, Applied Geophysics, 2nd ed., Cambridge University Press, UK.

Valenta, J., Stejskal, V. and Štěpančíková, P.: 2008, Tectonic pattern of the Hronov-Poříčí Trough as seen from pole-dipole geoelectrical measurements. Acta Geodyn. Geomater., 5, No. 2, 185–195.

Watson, D.: 1992, Contouring: A Guide to the Analysis and Display of Spatial Data. Pergamon Press, London.

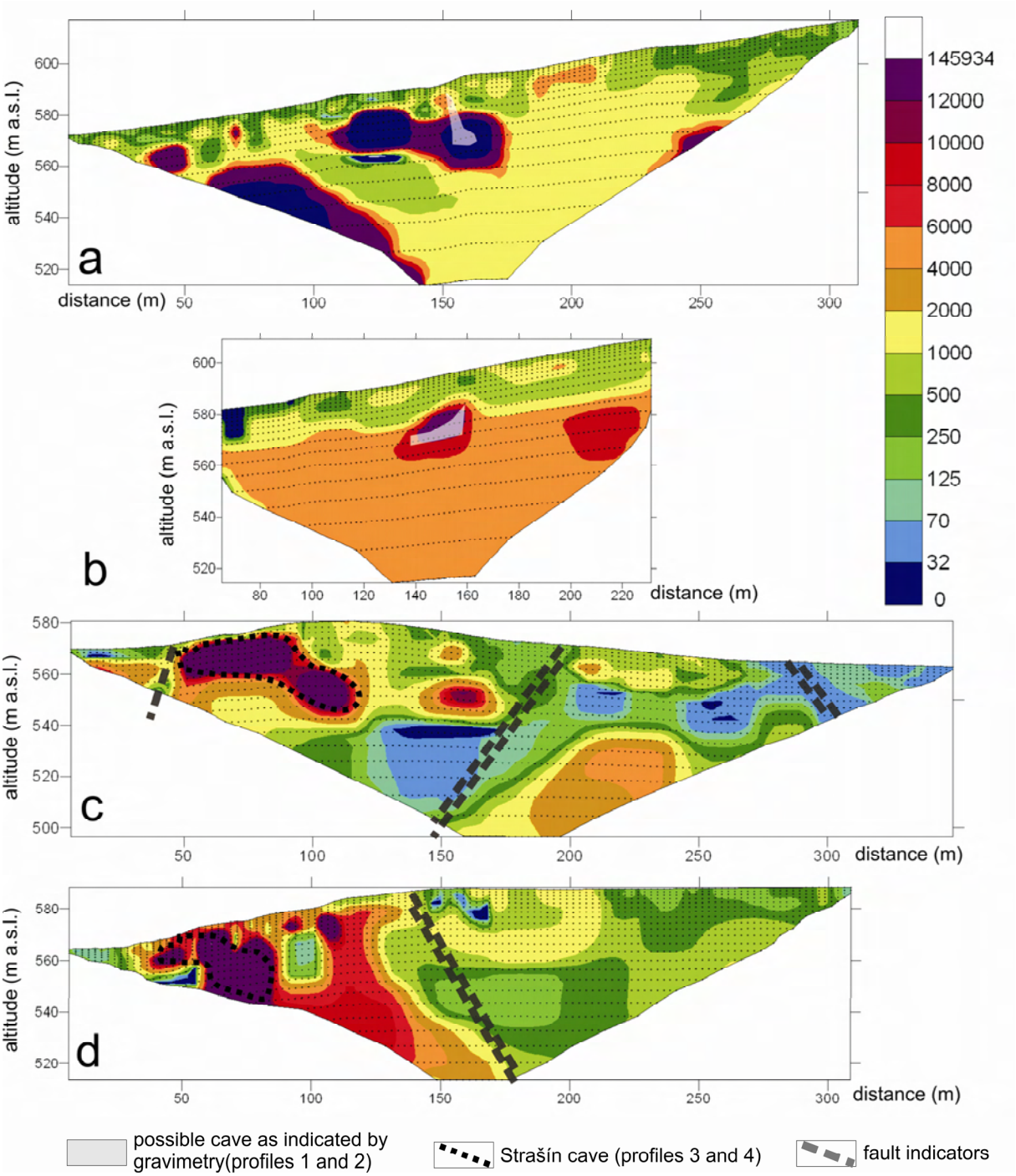


**Fig. 9** ERT profiles measured in the vicinity if Strašín cave showing the fault indications and caves. The scale represents values of apparent resistivity in Ωm. a) profile 1. The gravity anomaly is shown as semitransparent white shape, b) profile 2. The gravity anomaly is shown as semitransparent white shape, c) profile 3, d) profile 4.